CHAPTER 4

INFLUENCE OF SINTERING TEMPERATURE ON DIELECTRIC AND PIEZOELECTRIC PROPERTIES OF B_2O_3 DOPED $Ba(Ti_{0.9}Sn_{0.1})O_3$ CERAMICS

Lead-free ceramics of $Ba(Ti_{0.9}Sn_{0.1})O_3$ doped with B_2O_3 were prepared by a conventional solid state sintering method. Dielectric and piezoelectric properties of the ceramics were investigated as a function of sintering temperature. Although density of the ceramics was observed to decrease with increasing the sintering temperature, the sample sintered at 1350°C showed maximum dielectric constant for all doping conditions. However, the ceramics showed a lower piezoelectric coefficient (d_{33}) at a higher sintering temperature. The dielectric-electric field measurement indicated that this material exhibits a high tunability. In addition, mechanical property such as hardness was investigated. Relation between grain size and hardness of the ceramics was found to obey the Hall-Petch equation. Moreover, an increase in the boron oxide content was observed to enhance the hardness of the ceramics. These results may be helpful in the multilayer capacitor applications.

4.1 Introduction

Ferroelectric ceramics are very important for many electronic applications and many researchers have shown considerable interest in the electrical properties of these materials [1]. However, most of the commercial ceramics are lead-based compound

such as lead zirconate titanate (PZT) which has environmental problems due to lead oxide (PbO) present in the PZT causes pollution during preparation processing. Therefore, non-lead base ferroelectric ceramics such as modified $BaTiO_3$ and $Bi_{0.5}Na_{0.5}TiO_3$ have been widely investigated, because of their free control of sintering atmosphere and no release of lead in the process of fabrication [1-3]. In case of modified $BaTiO_3$ such as $Ba(Ti_{1-x}Sn_x)O_3$ (BTS), the high permittivity was observed for a composition $x \sim 0.1$ (BTS10). This material exhibits a diffuse phase transition with no relaxor ferroelectric behavior [3]. The Curie temperature can be controlled for various applications by varying the stannate molar fraction [4].

For multilayer capacitor applications, many researchers have focused on decreasing sintering temperature by adding some sintering aids such as Li_2O, Bi_2O_3 and B_2O_3 into their materials. These additives have been introduced into many modified $BaTiO_3$ ceramics to decrease the sintering temperature and improve their electrical properties [5]. However, the properties of some modified $BaTiO_3$ ceramics doped with B_2O_3 such as BTS have not been widely investigated. In the present work, BTS ceramics for the composition of BTS10 were prepared. The B_2O_3 was added into the BTS10 ceramics. Electrical properties of the resulting ceramics were studied and the effect of sintering temperature on the properties was also investigated.

4.2 Experimental

$Ba(Ti_{0.9}Sn_{0.1})O_3$ ceramics with B_2O_3 were prepared by a conventional ceramics fabrication method. Reagent grade of $BaCO_3$, SnO_2, and TiO_2 were mixed in isopropanol for 24 h using zirconia grinding media. Then, the slurry was dried, sieved

and calcined at 1300°C for 2 h. After calcination, B_2O_3 powder, equivalent to 0.50, 1.0, 2.0 and 3.0 wt.%, was added into BTS10 powder. The mixed powders with added organic binder were ball-milled in isopropanol for 24 h. The obtained slurry was dried and sieved to form a fine powder. Cylindrical pellets 15 mm in diameter were isostatically pressed at 80 MPa. The pellets were then sintered at 1250-1450°C for 4 h with a heating/cooling rate of 5°C/min. The samples for dielectric measurement were polished and electroded via gold sputtering. Phase formation of the ceramics was studied by X-ray diffraction analysis (XRD) with Cu Kα radiation. Microstructural evolution was investigated using scanning electron microscopy (SEM). The density and the apparent porosity of the sintered samples were determined by Archimedes' method with distilled water as the fluid medium. The dielectric properties were measured with an LCR meter. The piezoelectric coefficient (d_{33}) was measured with a d_{33} meter, 24 h after poling at 1.5 kV/mm. The surface hardness of the sintered samples was characterized by a Buehler Hardness Tester (Model No.1600-6100 Illinois, USA). Indentation was performed under a load of 100 N and maintained for 15 s.

4.3 Results and discussion

The phase evolution in the B_2O_3 doped BTS10 ceramics was determined from the X-ray diffraction patterns. Figure 4.1 and Figure 4.2 show XRD patterns of the 0.5 and 1.0 wt.% B_2O_3 doped BTS10 ceramics sintered at different temperatures.

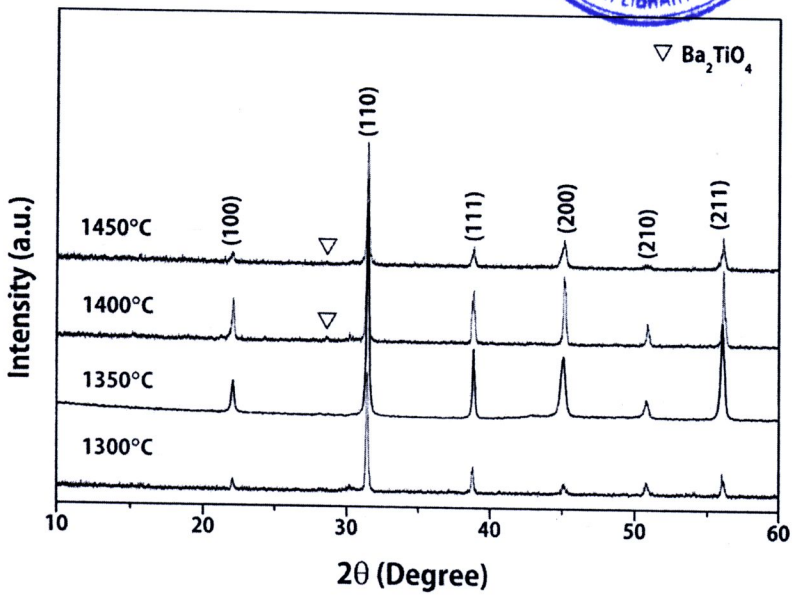

Figure 4. 1 X-ray diffraction patterns of 0.5 wt.% B_2O_3 doped BTS10.

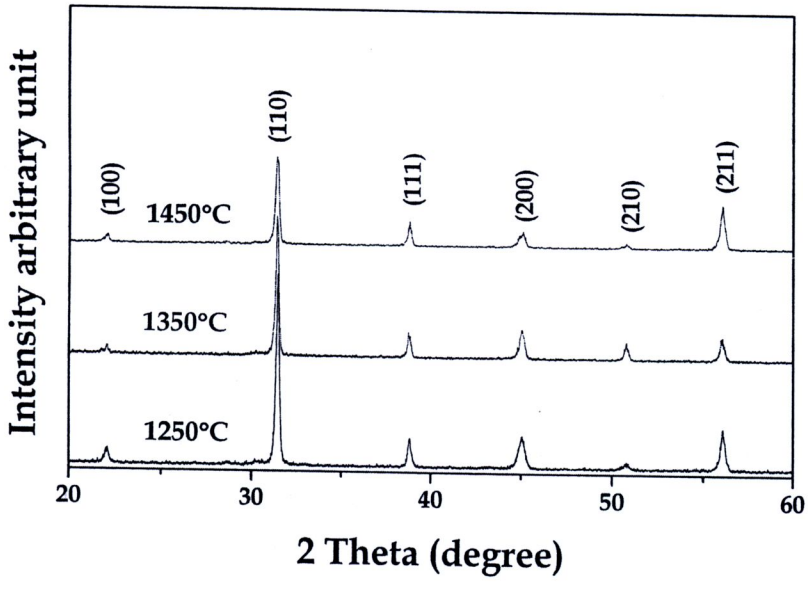

Figure 4. 2 X-ray diffraction patterns of 1.0 wt.% B_2O_3 doped BTS10.

A perovskite structure was observed for all samples. However at higher sintering temperature, a second phase was found as indicates in the Figure 4.1.

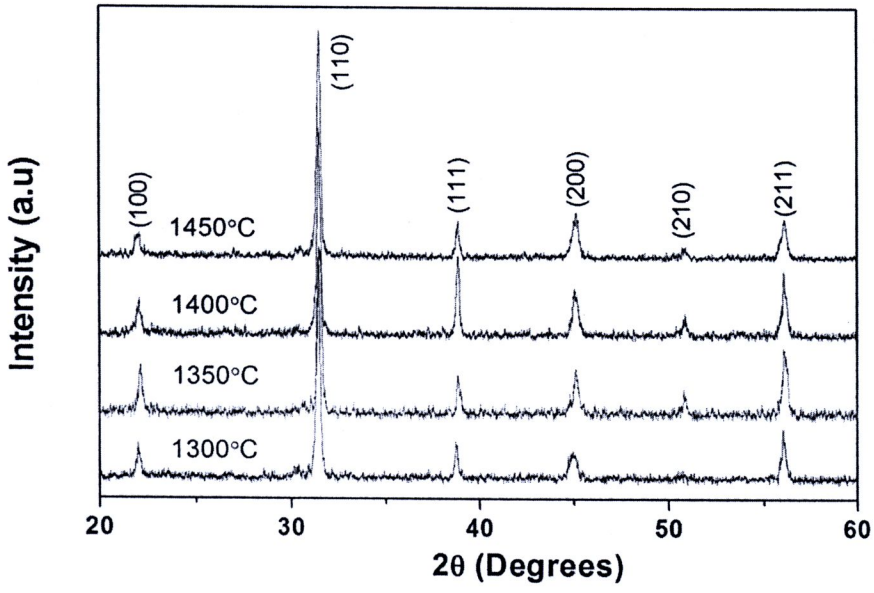

Figure 4. 3 X-ray diffraction patterns of 2.0 wt.% B_2O_3 doped BTS10.

Figure 4.3 shows XRD patterns of the 2.0 wt.% B_2O_3 doped BTS10 ceramic samples. The XRD patterns revealed that all samples exhibit a perovskite phase. Shift of XRD peaks was found, indicating a change of the lattice constant.

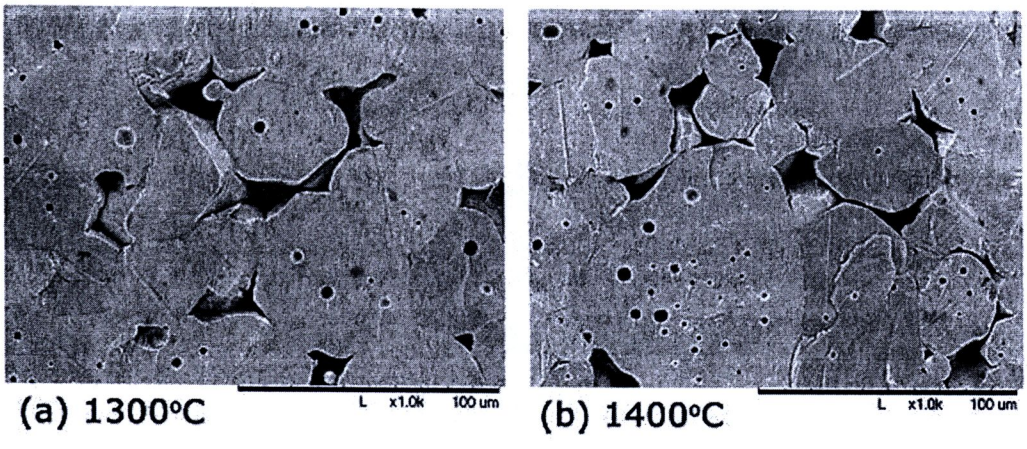

Figure 4. 4 SEM of the 0.5 wt.% B_2O_3 doped BTS10 ceramics.

The SEM micrographs of the 0.5 wt.% B_2O_3 doped BTS10 show that the higher sintering temperature produced a notable increase in grain size (Figure 4.4), especially at 1350°C. However, a decrease in density was also found for the samples sintered at higher temperature (Figure 4.5). It can be noted that the porosity levels evident in SEM micrographs of the pellet surfaces consist with trends in measured density values.

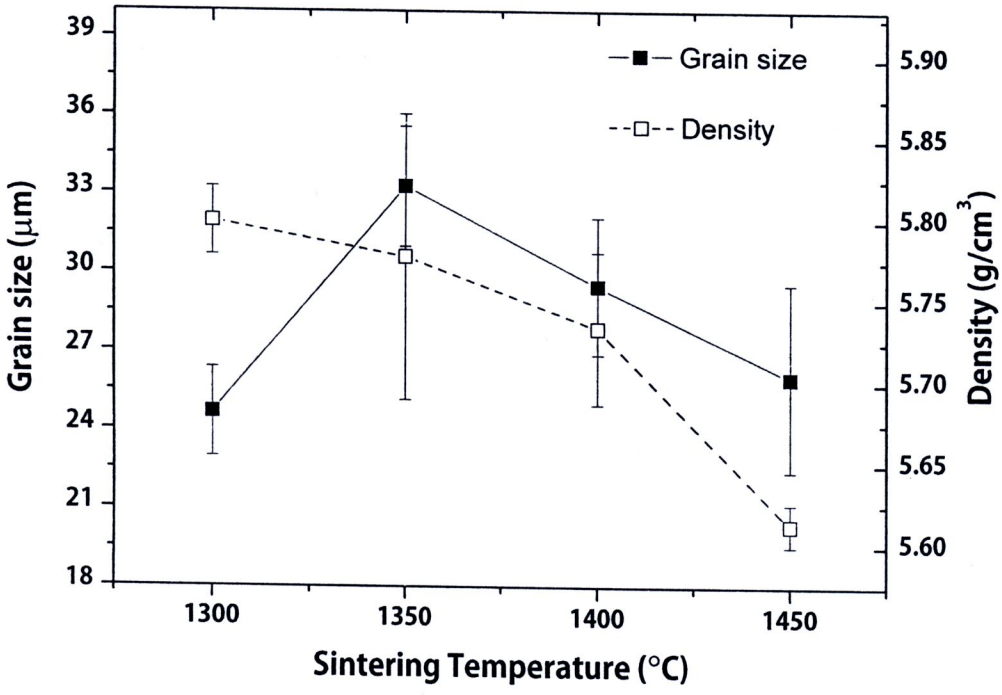

Figure 4. 5 Grain size and density as a function of sintering temperature for 0.5 wt.% B_2O_3 doped-BTS10 ceramics.

The density values of 1.0 wt.% B_2O_3 doped-BTS10 ceramics.as a function of sintering temperature are shown in Figure 4.6. The density increased with increasing sintering temperature up to 1300°C and then decreased for further sintering temperatures. It is expected that the presence of a B_2O_3 liquid phase assists

densification during sintering. However, high evaporation of B_2O_3 at high temperature may result in a lower final density.

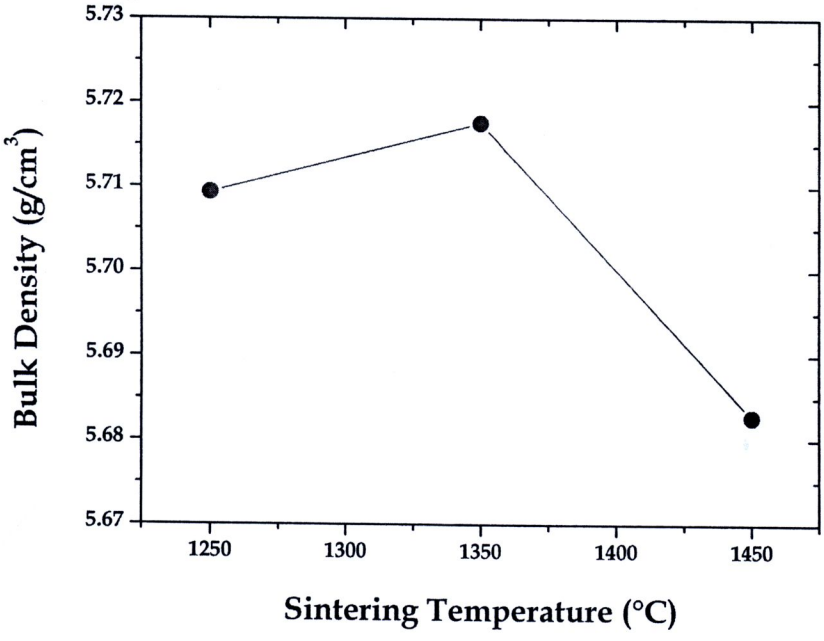

Figure 4. 6 Bulk density as a function of sintering temperature for 1.0 wt.% B_2O_3 doped-BTS10 ceramics.

SEM micrographs of the ceramics are illustrated in Figure 4.7. The porosity levels in SEM micrographs of the pellet surfaces were consistent with trends in measured density values. The microstructural analysis revealed that the increase of the sintering temperature enhances the grain size. Average values of grain size, as measured by the linear intercept method, increased from 26 μm for the sample sintered at 1250°C to 30 μm for the sample sintered at 1450°C.

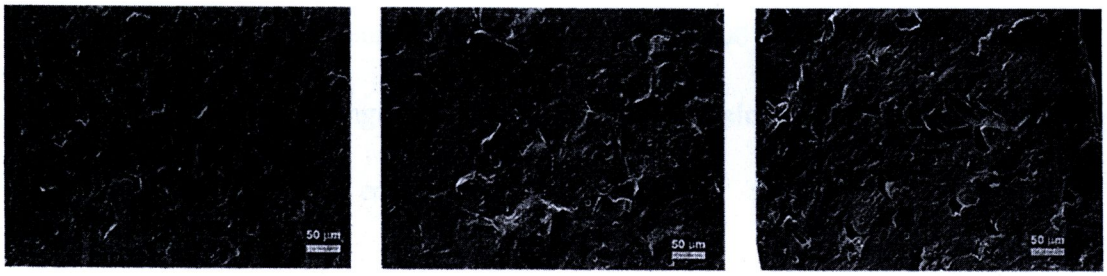

Figure 4. 7 SEM of the 1.0 wt.% B_2O_3 doped-BTS10 ceramics sintered at: (a)1250°C, (b)1350°C and (c)1450°C

The average grain size as a function of sintering temperature for 2.0 wt.% B_2O_3 doped-BTS10 ceramics.is shown in Figure 4.8. The grain size becomes much larger with higher sintering temperature.

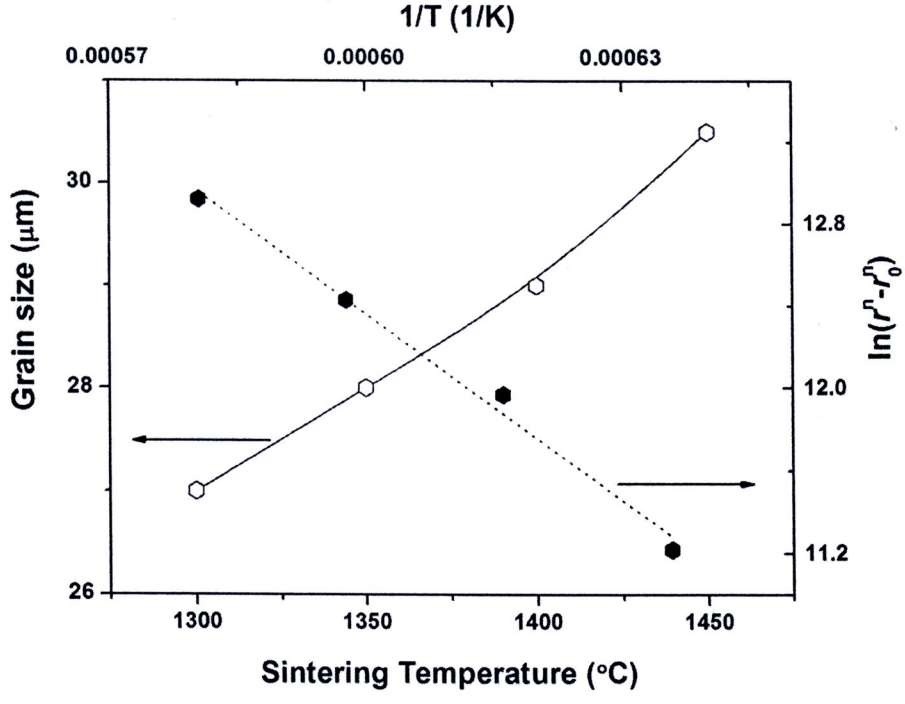

Figure 4. 8 Grain size as a function of sintering temperature for 2.0 wt.% B_2O_3 doped BTS10 ceramics.

The grain size increases from 27 μm for the 1300°C sample to 31 μm for the 1450°C sample. The change in the grain size with sintering temperature can be described by the Arrhenius equation as

$$r^n - r_0^n = k_0 exp\left(\frac{-\Delta H}{k_B T}\right) \tag{4.1}$$

where r_0 is the initial grain size, n is a growth exponent, k_0 is a constant, k_B is the Boltzmann constant, T is temperature in Kelvin and -ΔH is the activation energy. A plot of $\ln(r^n - r_0^n)$ as a function of reciprocal temperature is also shown in Figure 4.8. For n = 2, a linear relationship between $\ln(r^n - r_0^n)$ and $(1/T)$ was observed. From the slope of the curve in Figure 4.8, the activation energy has been determined to be about 2.61 eV.

The temperature dependence of the dielectric constant for the 0.5 wt.% B_2O_3 doped-BTS10 ceramics is shown in Figure 4.9. The maximum dielectric ($\varepsilon_{r,max}$) as a function of the sintering temperature is represented in the inset of Figure 4.9. Although the density was observed to decrease with sintering temperature, the maximum value of $\varepsilon_{r,max}$ of 9900 was found for the sample sintered at 1350°C with the phase transition temperature ~36°C. This sample displayed ~30% permittivity higher than the sample sintered at 1300°C (the base sample), indicates that adding B_2O_3 help to improve the dielectric permittivity of this material at a suitable sintering temperature.

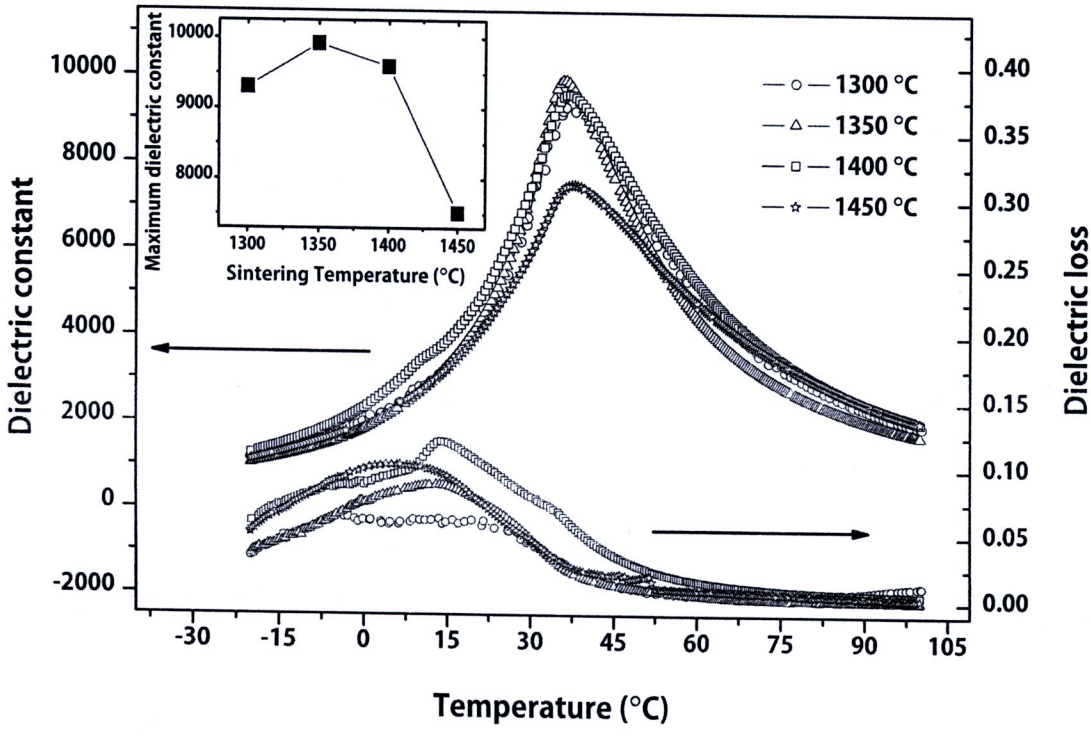

Figure 4. 9 Temperature dependence of the dielectric constant and loss for the 0.5wt.% B_2O_3 doped-BTS10 ceramics for various sintering temperatures

Figure 4.10 shows the dielectric constant as a function of temperature for the 1.0 wt.% B_2O_3 doped-BTS10 ceramics samples sintered for various temperatures at frequency 1 kHz. The results revealed that sintering temperature has an effect on the dielectric properties. There was an increase in peak dielectric constant from 6477 for the sample sintered at 1250°C to 13887 for the sample sintered at 1350°C, followed by reductions for the sample sintered at 1350°C (Table 4.1). This trend matches that of the sintered densities, i.e., the higher density samples gave higher measured dielectric constants. Figure 4.10 also shows the variation of dielectric loss as a function of temperature. The dielectric loss of our ceramics was less than 0.02. It was observed that the transition temperature of the samples is in the range of 34-36 °C.

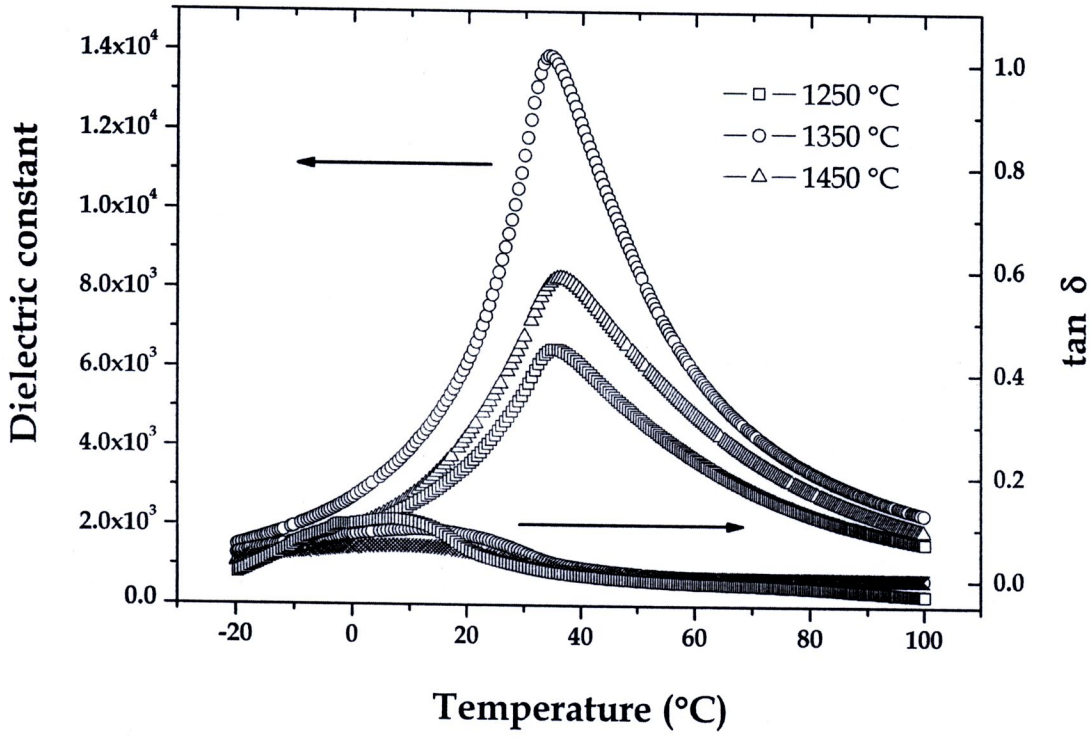

Figure 4. 10 Temperature dependence of the dielectric constant and loss for the 1.0wt.% B_2O_3 doped-BTS10 ceramics for various sintering temperatures

Although, sintering temperature has a significant effect on the grain size, but this factor has not influenced on the transition temperature (Table 4.1). Change in the piezoelectric constant (d_{33}) values as a function of the sintering temperature is shown in Table 4.1. The d_{33} coefficient was found to be in the range of 90-115 pC/N. However, the better d_{33} coefficient of 115 pC/N was observed for the sample sintered at 1250°C.

Table 4. 1 Electrical properties of 1.0 wt.% B_2O_3 doped-BTS10 ceramics.

Sintering temperature (°C)	$T_{c,max}$ (°C)	$\varepsilon_{r,max}$	Tanδ	d_{33} (pC/N)
1250	35.21	6477	0.0134	115
1350	34.15	13887	0.0345	107
1450	36.29	8281	0.019.	90

Figure 4.11 shows the dielectric constant and dielectric loss of the 2.0 wt.% B_2O_3 doped-BTS10 samples as a function of temperature. The dielectric maximum ($\varepsilon_{r,max}$) increases from 6800 for the 1300°C sample to 13900 for the1350°C sample, and then decreases to 10200 for the 1450°C sample.

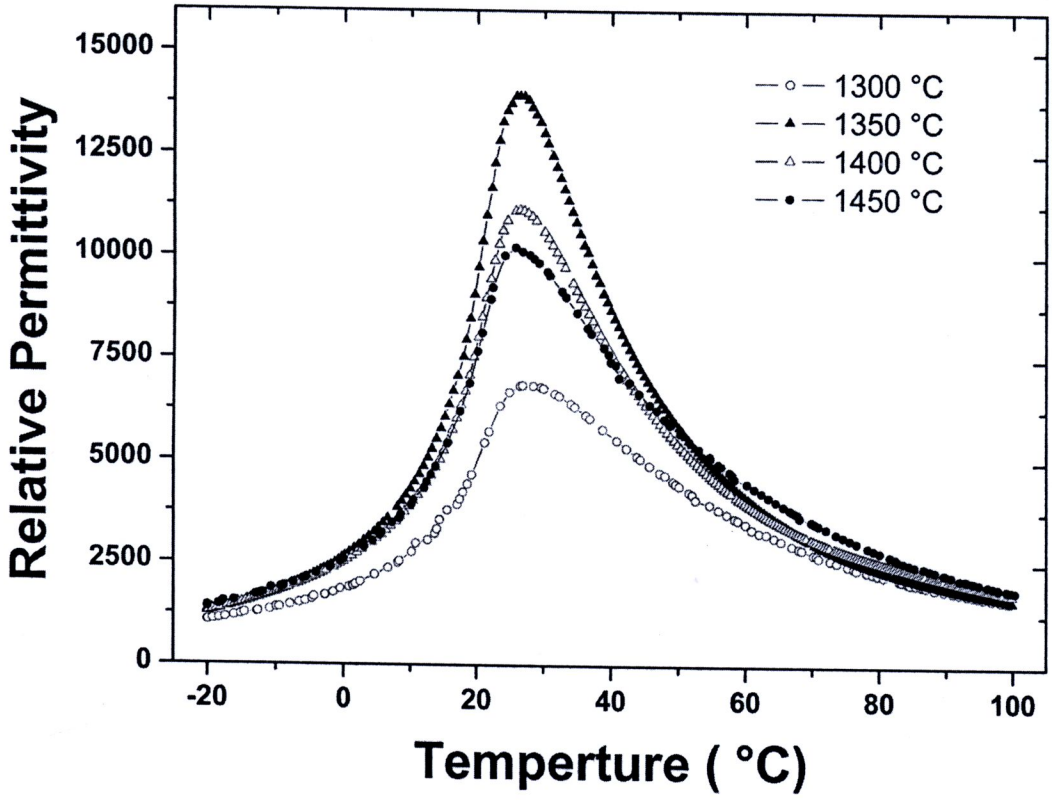

Figure 4. 11 Temperature dependence of the dielectric constant and loss for the 2.0wt.% B_2O_3 doped-BTS10 ceramics for various sintering temperatures.

It is noted that the highest dielectric maximum was observed at temperature of 26°C which is close to room temperature. Furthermore, the transition temperature has not changed much with sintering temperature (Figure 4.12), which indicates that this material can be used in electronic applications near room temperature.

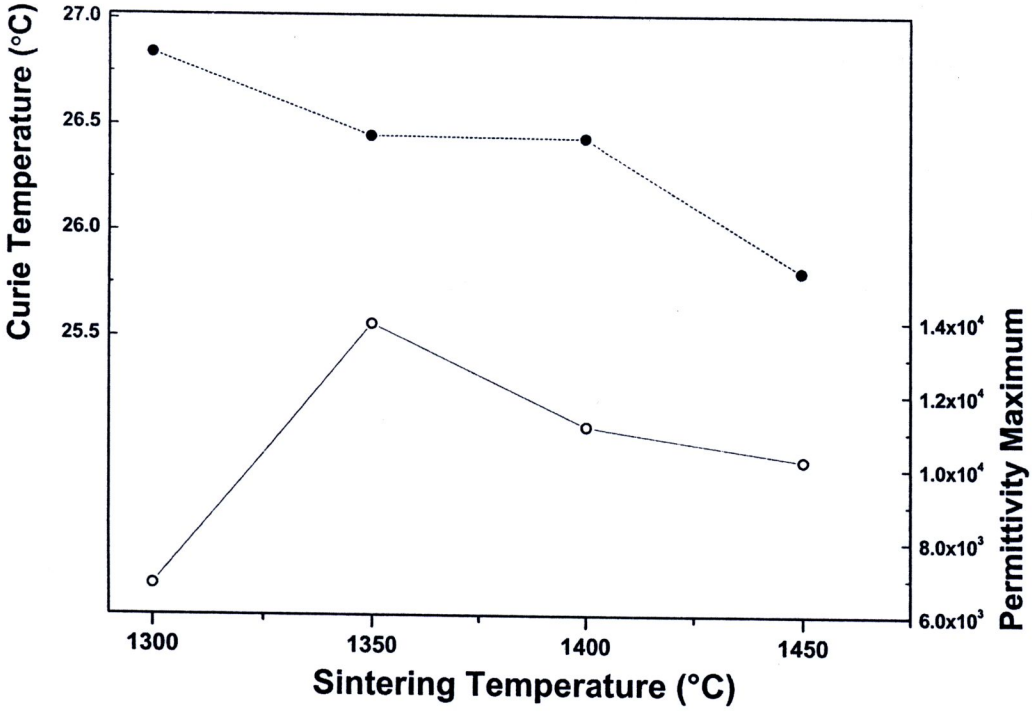

Figure 4. 12 T_{max} and $\varepsilon_{r,max}$ for the 2.0 wt.% B_2O_3doped-BTS10 ceramics.

It was proposed that the paraelectric side permittivity curve of ferroelectric with diffuse phase transition can be described by the expression:

$$\frac{\varepsilon_{r,max}}{\varepsilon_r} = exp\left[\frac{(T - T_m)^2}{2\delta_\gamma^2}\right] \tag{4.2}$$

where $\varepsilon_{r,max}$ is the maximum value of the relative dielectric constant at $T=T_m$, ε_r is the dielectric constant, and δ_γ is the diffuseness parameter of the transition. The value of δ_γ can be determined from the ln $(\varepsilon_{r,max}/\varepsilon_r)$ versus $(T- T_m)^2$ curve. This value is valid for $\varepsilon_{r,max}/\varepsilon_r < 1.5$, as clarified by Pilgrim et al.[6]. The values of parameter δ_γ are displayed in Figure 4.13. The parameter δ_γ was calculated to be 12.7 to 23.8°C. The lower parameter δ_γ of 12.7°C, indicates a sharp phase transition in the 1350°C sample.

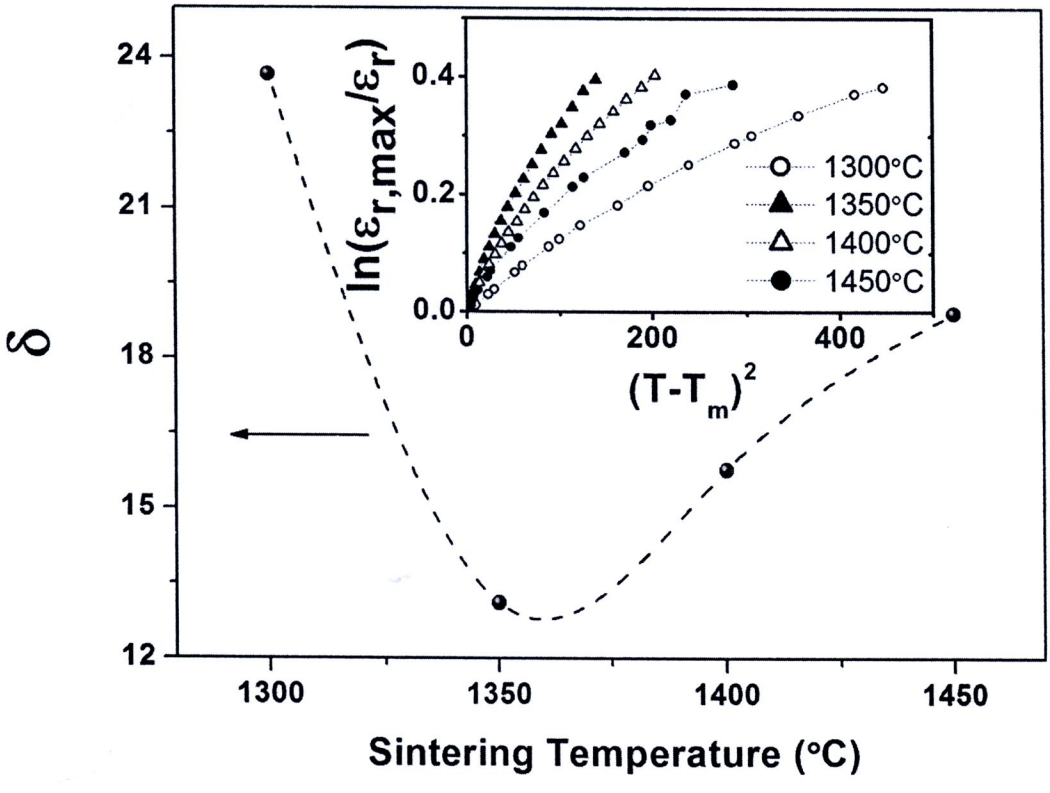

Figure 4. 13 Diffuseness parameter calculated from the ln $(\varepsilon_{r,max}/\varepsilon_r)$ versus $(T- T_m)^2$ curve

The dielectric properties at high electric field (E) were investigated in this work; Figure 4.14 shows the dielectric constant (ε_r) versus electric field (E) for the ceramics sintered at various temperatures. High tunability was observed in this material. Generally, the tunability can be defined as the ratio of the dielectric constant of the material at zero electric field to its dielectric constant at a higher electric field. Tunability coefficient n can be expressed here as

$$n = \frac{\varepsilon(0)}{\varepsilon(E)} \tag{4.3}$$

where $\varepsilon(0)$ and $\varepsilon(E)$ are the dielectric constant at zero and E electric field, respectively. In this work, $\varepsilon(E)$ was measured at 1.5 kV/mm.

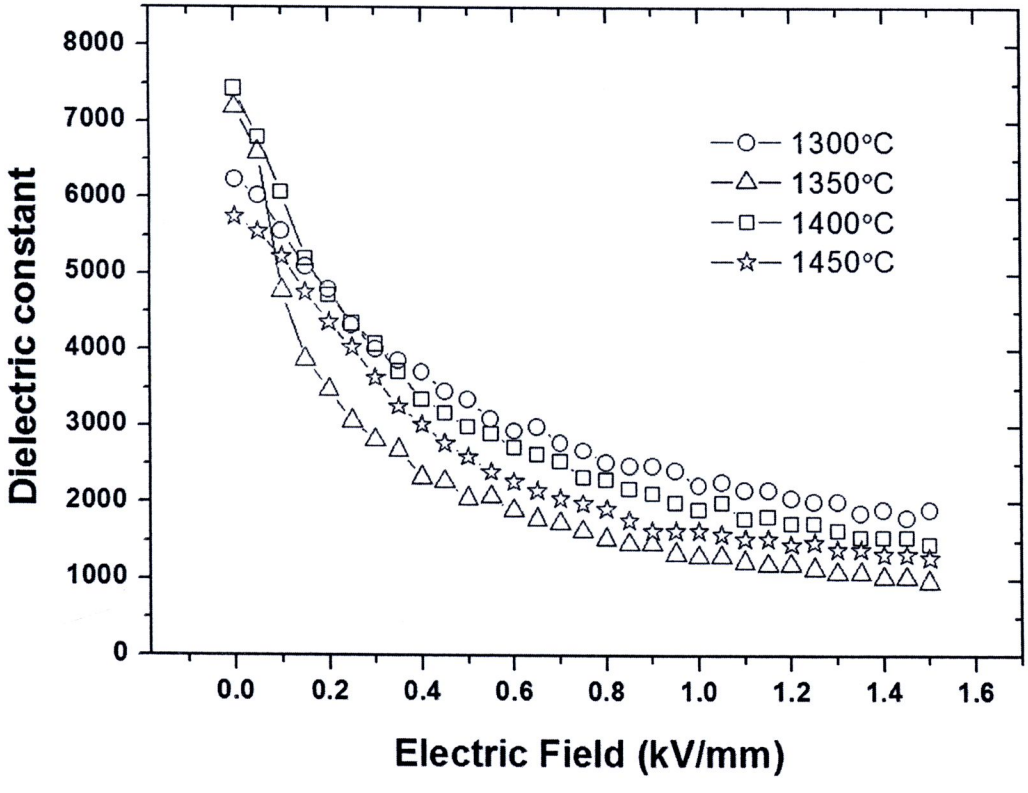

Figure 4. 14 ε_r-E characteristics of 0.5 wt.% B_2O_3 doped-BTS10 ceramics.

However, it can be defined the relative tunability (n_r) as

$$n_r = \frac{\varepsilon(0) - \varepsilon(E)}{\varepsilon(0)} \tag{4.4}$$

Plots of n and n_r versus sintering temperature of 0.5 wt.% B_2O_3 doped-BTS10 samples are shown in Figure 4.15. The 1350°C sample exhibits higher tunability and relative tunability (~83%). However, these values decrease for higher sintering temperature samples (1400-1450°C), due to the porosity effect.

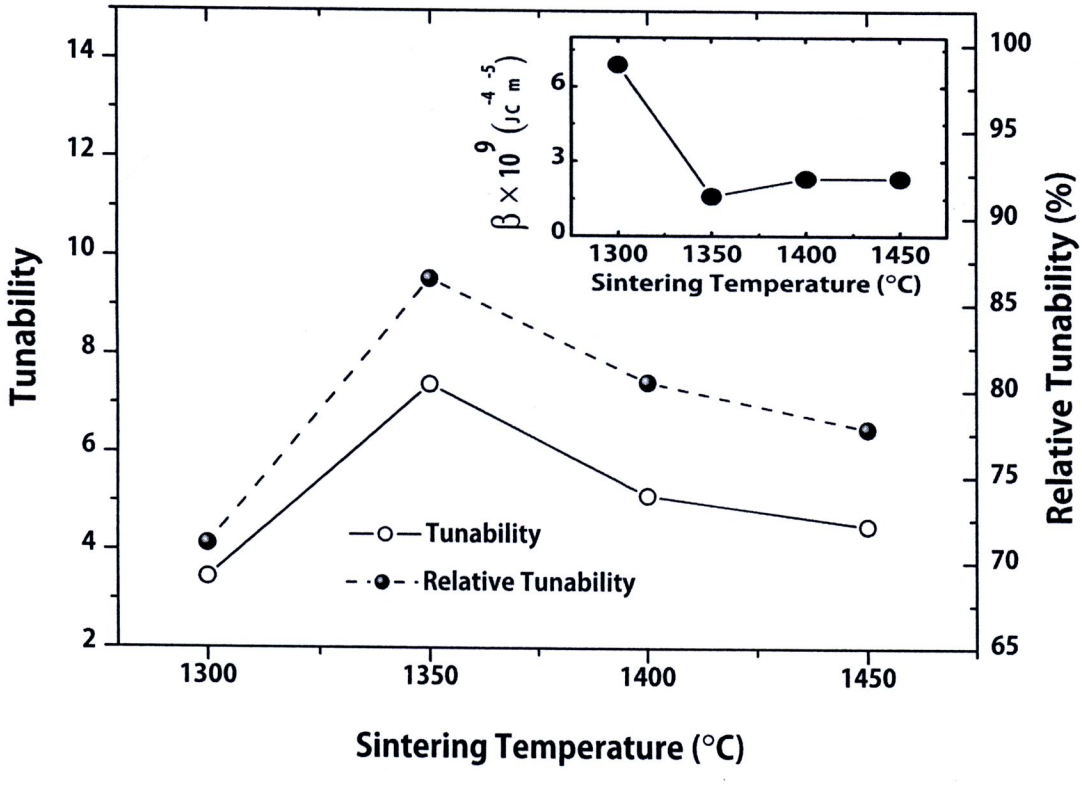

Figure 4. 15 Tunability and relative tunability measured of the 0.5 wt.% B_2O_3 doped-BTS10 ceramics sintered at various temperatures.

Venkatesh et al. [7] proposed that tunability is proportional to the nonlinear coefficient β and to the square of the electric field (at low field) which can be written as

$$n \approx 1 + 3\beta\left(\varepsilon_0 \varepsilon(0)\right)^3 E^2 \tag{4.5}$$

The value of β versus sintering temperature is shown in the inset of Figure 4.15. It can be seen that β decreases for the higher sintering temperature samples, indicating that this parameter depend on material processing.

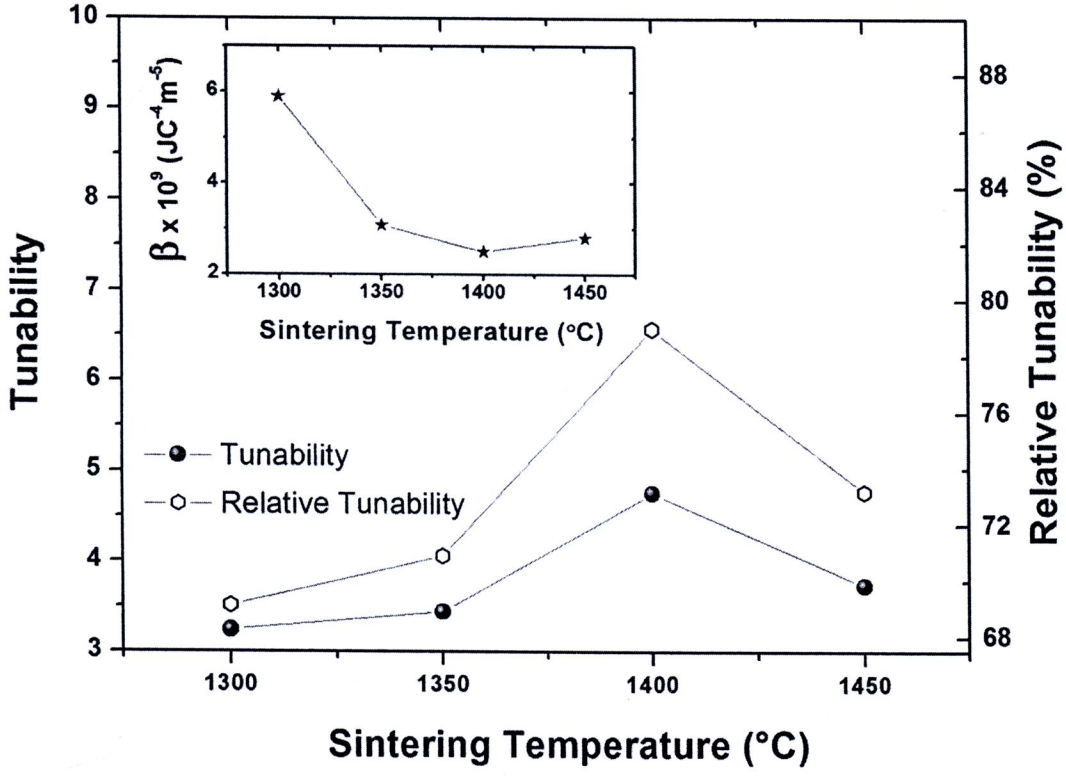

Figure 4. 16 Tunability and relative tunability measured of the 2.0 wt.% B_2O_3 doped-BTS10 ceramics sintered at various temperatures.

Plots of n and n_r versus sintering temperature of 2.0 wt.% B_2O_3 doped-BTS10 samples are shown in Figure 4.16. A high relative tunability of ~ 83% was observed in the 1400°C sample. However, this value decreases for higher sintering temperature samples (1450°C).

Figure 4.17 shows the piezoelectric coefficient (d_{33}) as a function of sintering temperature. The d_{33} value decreases with increasing the sintering temperature.

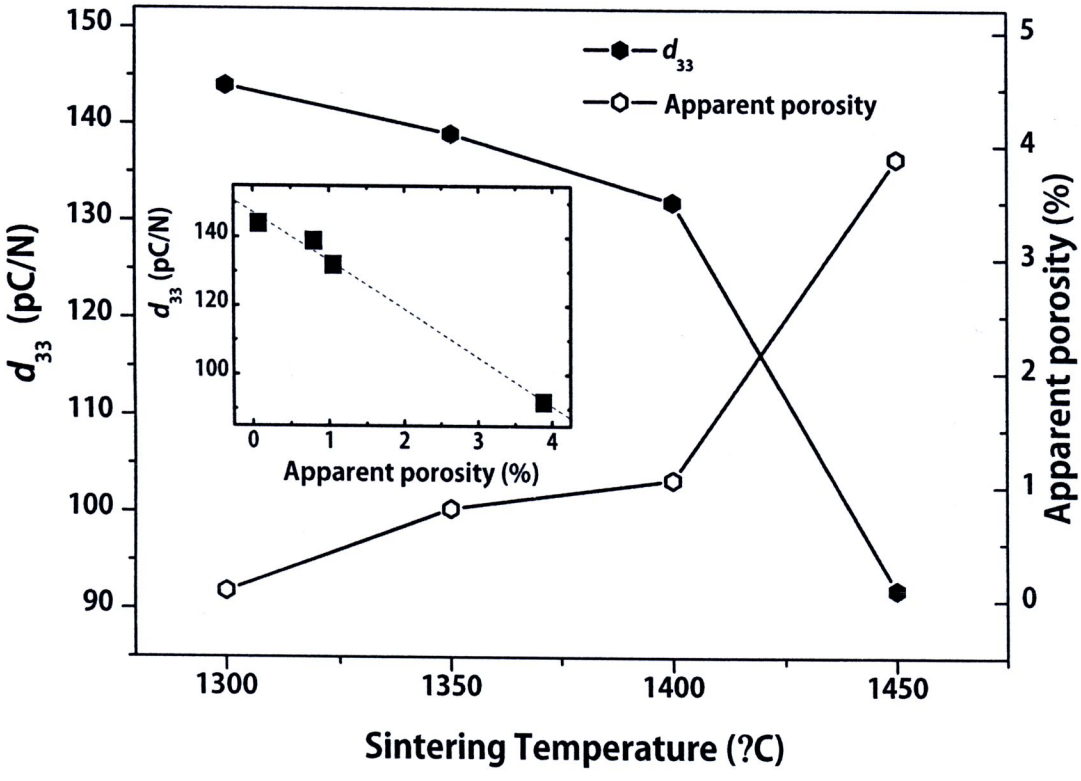

Figure 4. 17 Piezoelectric constant (d_{33}) of BTS10 ceramics doped with 0.5 wt.% B_2O_3 for various sintering temperatures.

Again, the lower d_{33} value is likely due to the higher porosity (inset of Figure 4.17) in the samples sintered at higher temperature. The d_{33} as a function of apparent porosity can be expressed as

$$d_{33} = -1.47P + 147 \tag{4.6}$$

where P is apparent porosity. The higher porosity in samples sintered at higher temperature also made the ceramics easy to break down and difficult to pole at high electric field.

In this work, hardness was also investigated since it is important for some applications that these ceramics are resistant to fracture toughness or microcracking when subjected to large electric fields. The hardness values of 2.0 wt.% B_2O_3 doped-BTS10 for all of the samples are shown in Figure 4.18. It can be seen that the higher sintering temperature produced a slight decrease in hardness value. However, the hardness value can be related to the grain size. A plot of the hardness as a function of grain size is shown in the inset of Figure 4.18. A linear relation between hardness and grain size$^{-1/2}$ of the ceramics was observed which can be expressed as

$$H_V = 0.07 + 12.9G^{-\frac{1}{2}} \tag{4.7}$$

where H_v is hardness and G is grain size. The result indicates that the hardness values of our ceramics obey the Hall–Petch equation.

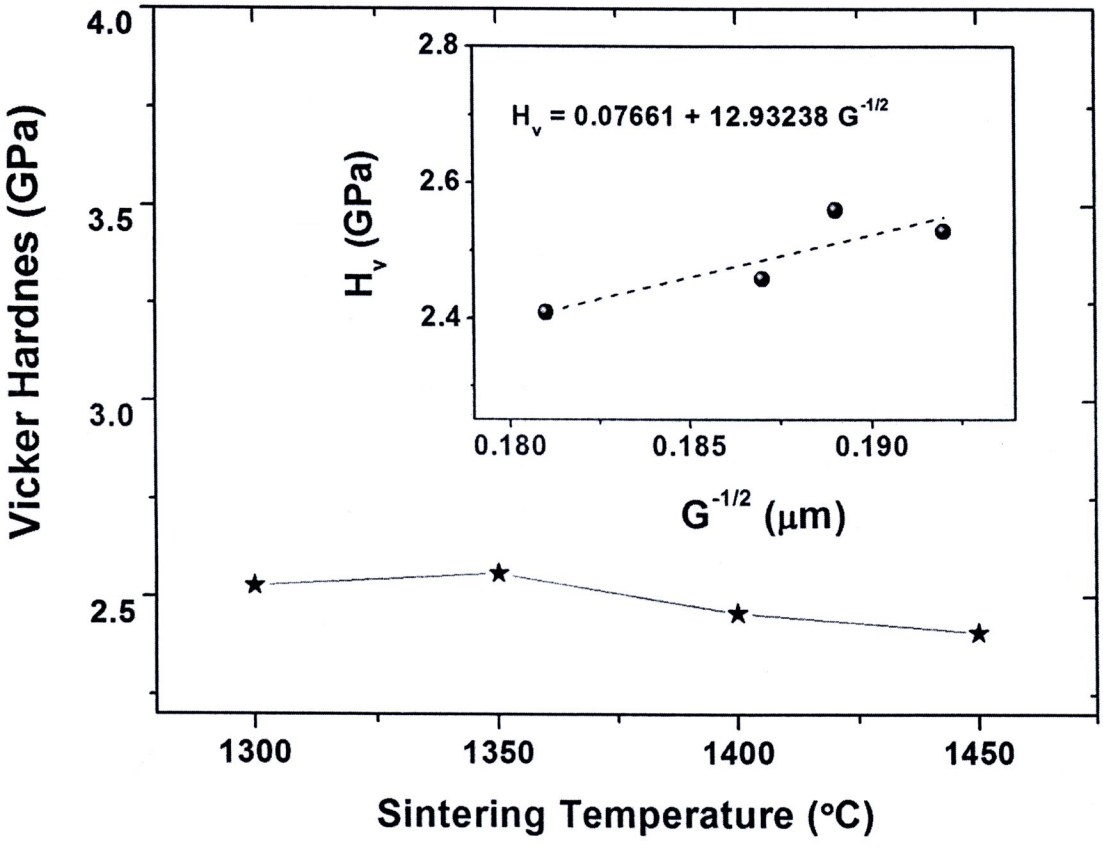

Figure 4. 18 Sintering temperature dependence of Vicker hardness.

4.5 Conclusions

Properties of BTS10 doped with B_2O_3 sintered at various temperatures were investigated. The XRD patterns showed the perovskite phase in all samples. All samples exhibited high tunability. The higher $\varepsilon_{r,max}$ and tunability were found for the samples sintered at 1350°C. However, the relative tunability decreased for the sintering temperature at 1450°C. In addition, high sintering temperature samples showed a significant fall in d_{33} coefficient due to the porosity effect and produced a slight decrease in hardness value either. These results may be useful in the development of lead free capacitor applications.

4.6 References

[1] K. Pengpat, S. Hanphimol, S. Eitssayeam, U. Intatha, G. Rujijanagul, T. Tunkasiri, Morphotropic phase boundary and electrical properties of lead-free bismuth sodium lanthanum titanate—barium titanate ceramics, Journal of Electroceramics, 16 (2006) 301-305.

[2] Y. Lu, Y. Li, D. Wang, Q. Yin, Morphotropic phase boundary and electrical properties of $(Bi_{1/2}Na_{1/2})TiO_3$-$(Bi_{1/2}K_{1/2})TiO_3$-$(Bi_{1/2}Ag_{1/2})TiO_3$ ceramics, Ferroelectrics, 358 (2007) 109-116.

[3] W. Xiaoyong, F. Yujun, Y. Xi, Dielectric relaxation behavior in barium stannate titanate ferroelectric ceramics with diffused phase transition, Applied Physics Letters, 83 (2003) 2031-2033.

[4] Y.L. Tu, J.M. Herbert, S.J. Miline, Fabrication and characterization of high permittivity ceramics in the $Ba(Ti_{1-x-y}Sn_xZr_y)O_3$ system, Journal of Materials Science, 29 (1994) 4152-4156.

[5] S.M. Rhim, S. Hong, H. Bak, O.K. Kim, Effects of B_2O_3 addition on the dielectric and ferroelectric properties of $Ba_{0.7}Sr_{0.3}TiO_3$ ceramics, Journal of the American Ceramic Society, 83 (2000) 1145-1148.

[6] S.M. Pilgrim, A.E. Sutherland, S.R. Winzer, Diffuseness as a useful parameter for relaxor ceramics, Journal of the American Ceramic Society, 73 (1990) 3122-3125.

[7] J. Venkatesh, V. Sherman, N. Setter, Synthesis and dielectric characterization of potassium niobate tantalate ceramics, Journal of the American Ceramic Society, 88 (2005) 3397-3404.